The Effect of Viscosity Ratio on the Phase Inversion of Polyamide 66/Polypropylene Blends

PIRJO T. HIETAOJA,[1] RIITTA M. HOLSTI-MIETTINEN,[1,*] JUKKA V. SEPPÄLÄ,[1] and OLLI T. IKKALA[2]

[1]Helsinki University of Technology, Department of Chemical Engineering, Kemistintie 1, SF-02150 Espoo, Finland; [2]Neste Oy, P.O.B. 310, SF-06101 Porvoo, Finland

SYNOPSIS

The rheological properties of the blend components are an important parameter in the formation of a blend morphology. The effect of viscosity ratio on the morphology of polyamide 66/polypropylene blends was studied, with primary attention to the phase-inversion behavior and the average particle size of the dispersed phase. The relationship between the mechanical properties and the phase-inversion composition was investigated as well. Noncompatibilized and compatibilized blends having five different viscosity ratios were prepared by twin-screw extrusion. Maleic anhydride-grafted polypropylene was used as the compatibilizer to increase the adhesion between the two polymers and to stabilize the blend morphology. Investigation of the morphology of the blends by microscopy (SEM and TEM) showed that the smaller the viscosity ration (η_{PA}/η_{PP}) the smaller was the polyamide 66 concentration at which the phase inversion took place and that polyamide 66 became the continuous phase. The results are in accord with the model of Jordhamo. The compatibilizer induced a sharp reduction of particle size, but did not have a major effect on the phase-inversion point. The tensile and impact properties of the compatibilized blends were found to correlate with the phase inversion. An improvement in the mechanical properties was observed when polyamide 66 provided the matrix phase.

INTRODUCTION

The morphology strongly affects the macroscopic properties of a blend, which means that it is important to control the size and shape of the dispersed phase. The morphology of immiscible polymer blends is created during mixing and is affected by the blending conditions, interfacial tension between the components, specific interactions such as possible covalent or hydrogen bonding, and the viscosity ratio of the components.[1-3]

Normally, the major component forms the continuous phase.[4] When the volume fraction of the dispersed phase is increased, the average particle size increases as well. At approximately 50/50 composition, co-continuity of the two phases is observed. In addition to the composition, the phase-inversion point also depends on the viscosity of the components under the conditions of blending. The component with the lowest viscosity tends to form the continuous phase.[5]

The dependence of the morphology on the ratio of the viscosity of the dispersed phase to the viscosity of the matrix ($p = \eta_d/\eta_m$) has earlier been investigated by Wu,[6] who studied the droplet deformation and breakup for blends of polyamide or poly(ethylene terephthalate) with ethylene–propylene elastomers. He found that the relative influence of interfacial tension and viscosity ratio on phase morphology dimensions can be characterized with a dimensionless Weber number:

$$We = \frac{\eta_m \dot{\gamma} r}{\gamma_{12}} = 4\left(\frac{\eta_d}{\eta_m}\right)^{\pm 0.84} \quad (1)$$

where $\dot{\gamma}$ is the shear rate, r, the radius of the dispersed particle; and γ_{12}, the interfacial tension. The exponent is positive if the viscosity ratio η_d/η_m is > 1 and negative if the viscosity ratio is < 1. The diameter of the dispersed particles at equilibrium is

* To whom the correspondence should be addressed.

Journal of Applied Polymer Science, Vol. 54, 1613–1623 (1994)
 CCC 0021-8995/94/111613-11

directly proportional to the interfacial tension and inversely proportional to the shear rate and matrix viscosity for a given viscosity ratio. These equations indicate that smallest particles are generated when the viscosity ratio is near unity. Serpe et al.[7] showed eq. (1) to be valid for polyamide/polyethylene blends.

The effect of the viscosity ratio, p, on the size of the dispersed minor phase in polypropylene/polycarbonate blends has been studied in the regions $p > 1$ and $p < 1$ by Favis and Chalifoux.[8] The ratio had a marked effect on the morphology of the dispersed phase, with the phase size increasing by a factor of 3–4 as p was increased from 4.5 to 17.3. The size of the minor phase was reduced when the viscosity ratio was below unity, with the minimum size achieved at $p = 0.15$. At high viscosity ratios, the processing environment comes to play an important role. At $p = 17.3$, the phase size was four times as large in an internal mixer as in a twin-screw extruder. At lower viscosity ratios, the morphologies obtained with the two different compounding techniques were identical.[9]

The relationship between the phase size and composition has been studied in polypropylene/polyamide and polyethylene/polyamide blends by Willis et al.[10] The particle size of the noncompatibilized blends increased with the minor phase concentration, but the correlation was less pronounced when an ionomer was added as the compatibilizer.

Although polymer viscosities are temperature-dependent, according to Dagli et al.[11] the mixing temperature does not significantly affect the viscosity ratio in polyamide/polypropylene blends. However, there is a clear dependence of the viscosity ratio on the shear rate. Evaluation of the shear rate applied under the circumstances of blending is thus of crucial importance.

Through an optimal choice of blend components, it is possible to tailor the blend so that the polymer with better properties forms the continuous phase. In this work, we studied the effect of the viscosity ratio on the phase inversion of polyamide 66/polypropylene blends. The viscosity ratio was varied by using five polypropylenes with different melt viscosities. Both noncompatibilized and compatibilized blends were prepared. A graft copolymer compatibilizer was added to increase interactions through new covalent bondings between the phases.

EXPERIMENTAL

Materials

One polyamide 66 (PA66) and five different grades of polypropylene (PP) provided the polymers. Polyamide 66 Ultramid A3 was supplied by BASF and polypropylenes VA4020E, VB6511B, VC1812H, VC3512H, and VC5076ENA were supplied by Neste. The compatibilizer was PP grafted with 0.4 wt % maleic anhydride (PP-*g*-MAH).

Blending and Injection Molding

PA66 was dried for 16 h at 80°C before melt blending. Blends were prepared by melt-blending with a corotating twin-screw extruder Berstorff ZE 25. The rotation speed was 200 rpm and the melt temperature 270–278°C. The extrudate was immediately quenched in a water bath. Samples for microscopic investigations were taken before pelletizing.

PA66/PP blends were prepared in compatibilized and noncompatibilized form in the weight ratios 20/80, 30/70, 40/60, 50/50, 60/40, 70/30, and 80/20. The amount of the compatibilizer, PP-*g*-MAH, was in all cases 5 wt % of the total blend weight. The compatibilizer was also added to the pure polymers.

The compatibilized blends and compatibilized pure polymers were injection-molded into the form of test specimens after drying with an Engel ES 200/40. Blends were injection-molded at the melt temperature of 250–280°C, and the compatibilized pure PPs, at 210–230°C. Other injection-molding conditions were kept constant for all blends.

Characterization

A systematic characterization of the blends was undertaken by rheological, microscopic, and mechanical analysis. Melt viscosities were measured at 280°C with a Göttfert Rheograph 2002 capillary rheometer with capillary length/diameter ratio of

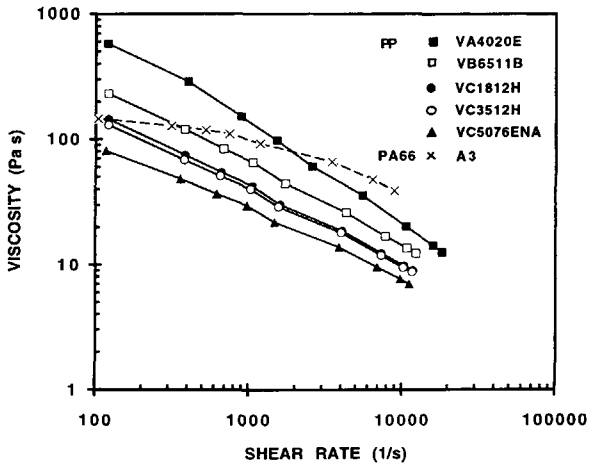

Figure 1 Melt viscosities of PA and PPs vs. shear rate at 280°C.

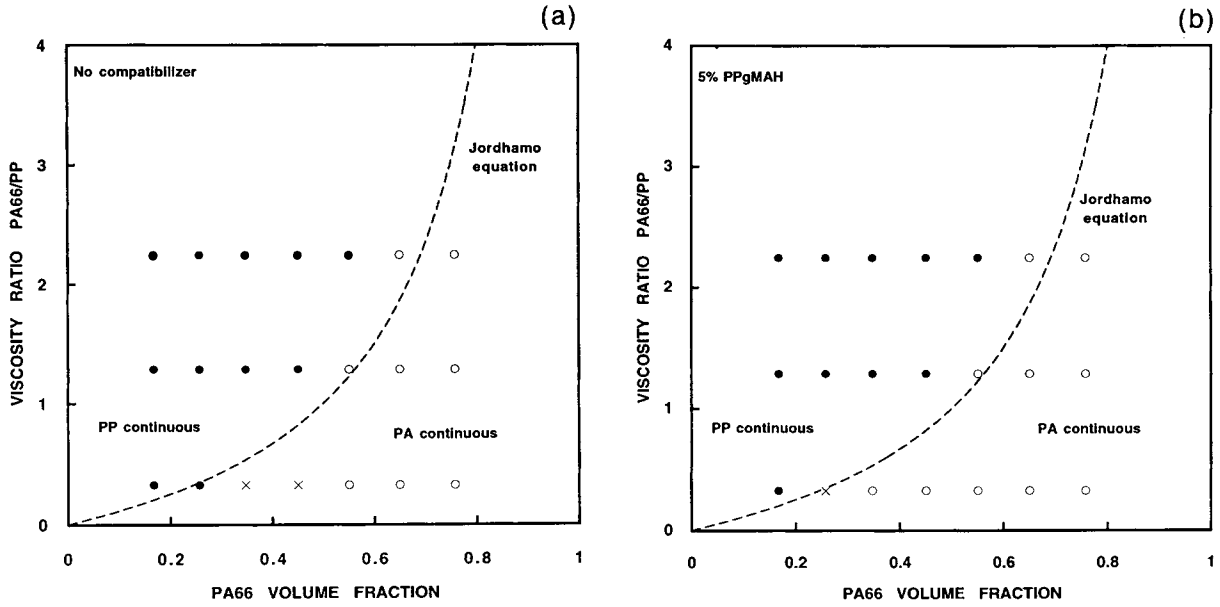

Figure 2 The phase-inversion regions of the blends as a function of viscosity ratio and PA composition containing (a) 0 wt % compatibilizer or (b) 5 wt % compatibilizer. Continuous phase is (●) PP or (○) PA or (X) dual phase continuity is seen. (– – –) Jordhamo's model.

20/1. PA66 and the blends were predried at 80°C for 16 h. Rabinowitch correction was made.

Blend morphology was investigated with a scanning electron microscope (SEM) JEOL JSM-820 and a transmission electron microscope (TEM) JEOL JEM 1200EX II. Micrographs were taken of twin-screw extrudates. The samples for SEM were prepared by fracturing the extrudate at liquid nitrogen temperature and were gold-coated before microscopy. For TEM, the samples were cut into thin sections with a microtome and stained with ruthenium hypochlorite.

Reichert-Jung 2050 microtome equipment was used to prepare thin samples from the extrudate. The phase-inversion region of the noncompatibilized blends was investigated for these samples with the Leitz Laborlux 12 POL S light microscope and the Mettler FP 82 hot stage. The melting of each polymer phase was observed and the continuous and dispersed phases were characterized.

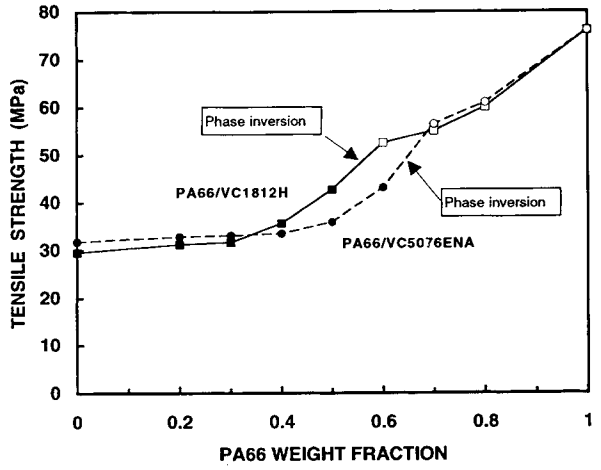

Figure 3 The maximum tensile strength of the compatibilized blends (□, ■) PA/PP VC1812H and (○, ●) PA/PP VC5076ENA as a function of PA composition. Continuous phase is (●, ■) PP or (○, □) PA.

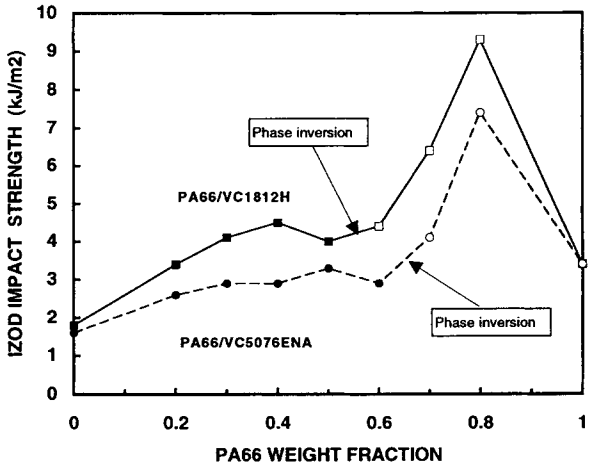

Figure 4 The notched Izod impact strength of the compatibilized blends (■, □) PA/PP VC1812H and (●, ○) PA/PP VC5076ENA as a function of PA composition. Continuous phase is (●, ■) PP or (○, □) PA.

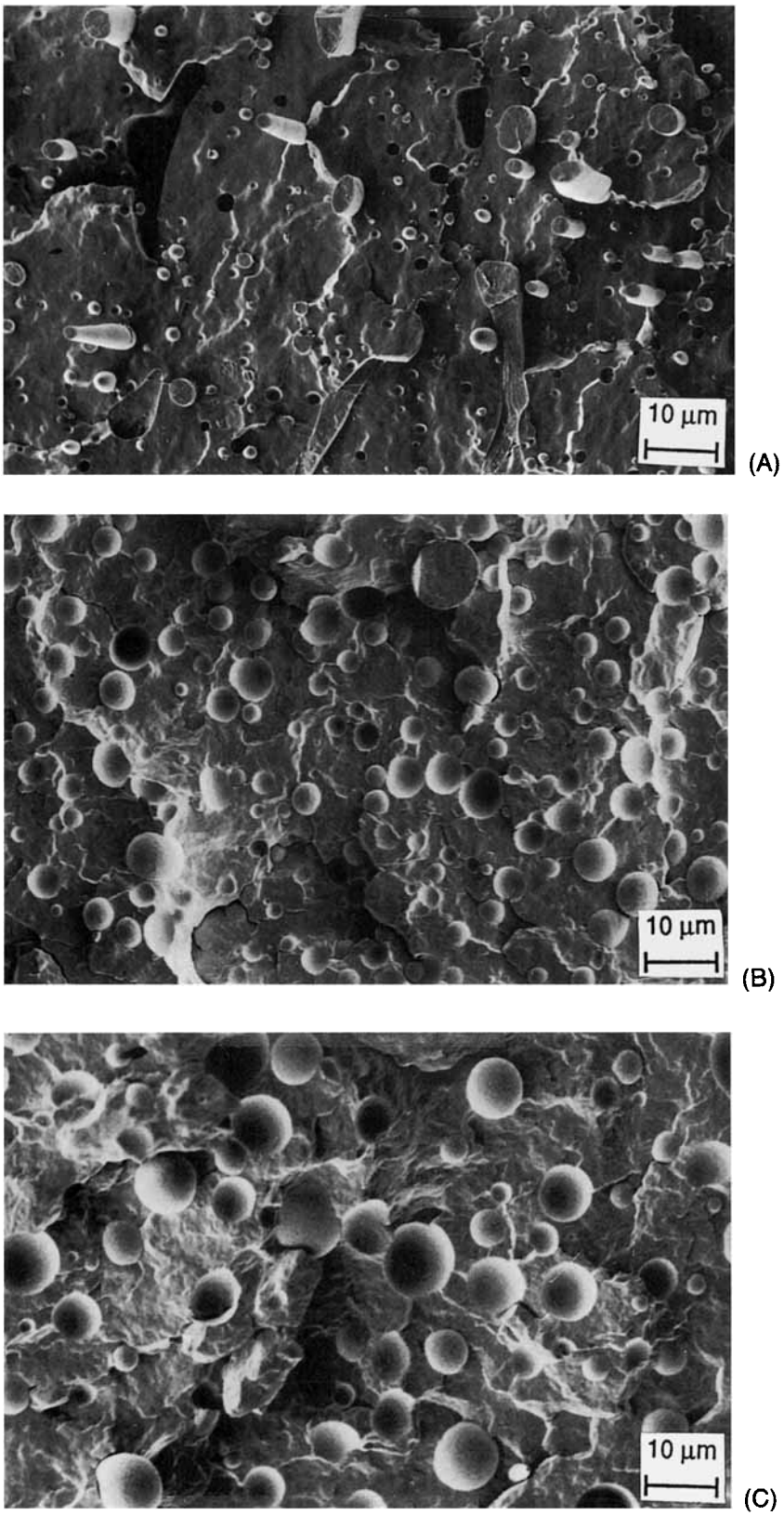

Figure 5 SEM photographs from blends (A) PA 20/PP VA4020E 80, (B) PA 20/PP VB6511B 80, (C) PA 20/PP VC1812H 80, (D) PA 20/PP VC3512H 80, and (E) PA 20/PP VC5076ENA 80.

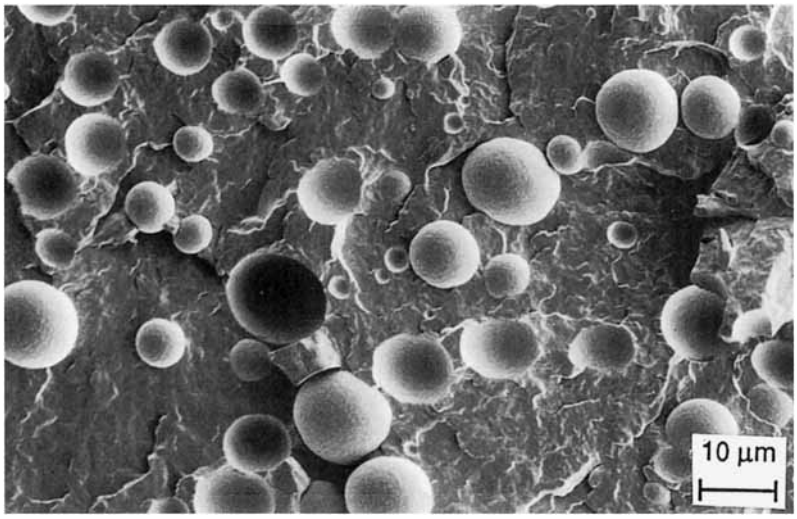

(D)

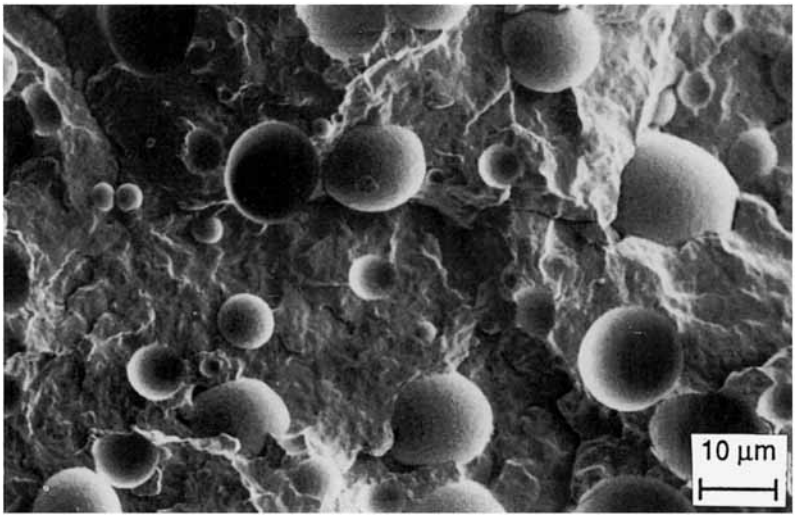

(E)

Figure 5 (*Continued from the previous page*)

Injection-molded samples were predried for 16 h at 80°C before mechanical testing and preserved in an desiccator until measured. A minimum of five samples was tested in each case.

Tensile properties were measured with an Instron 4204 testing machine at 23°C according to ISO R 527. The strain rate was 10 mm/min. The maximum tensile strengths were evaluated from the stress–strain data. Flexural properties were studied with the same equipment, by the three-point-bending test, according to ISO 178. The test speed was 10 mm/min. The notched Izod impact strength was determined with a Zwick 5102 testing machine according to ISO 180/1A.

RESULTS AND DISCUSSION

Viscosities of Component Polymers

The melt viscosities of the polymers are presented as a function of shear rate in Figure 1. Since the measuring temperature was the same as the blending temperature, 280°C, the measured viscosities indicate the viscosities that dominated under the processing conditions. The shear thinning behavior of PP was more noticeable than that of PA. At higher shear rates, the viscosity of the PA that we used is higher than that of the PPs. The viscosity ratios of PA to PP varied from about 0.3–5 in the range of

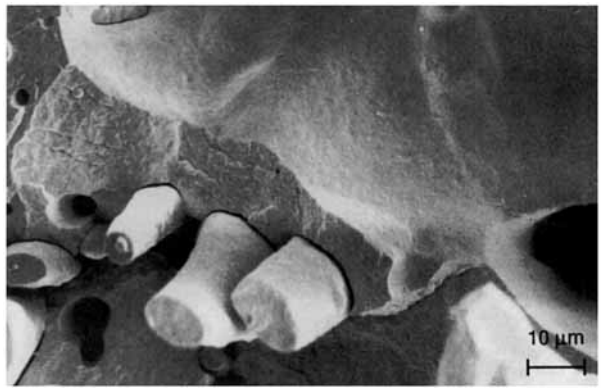

(A)

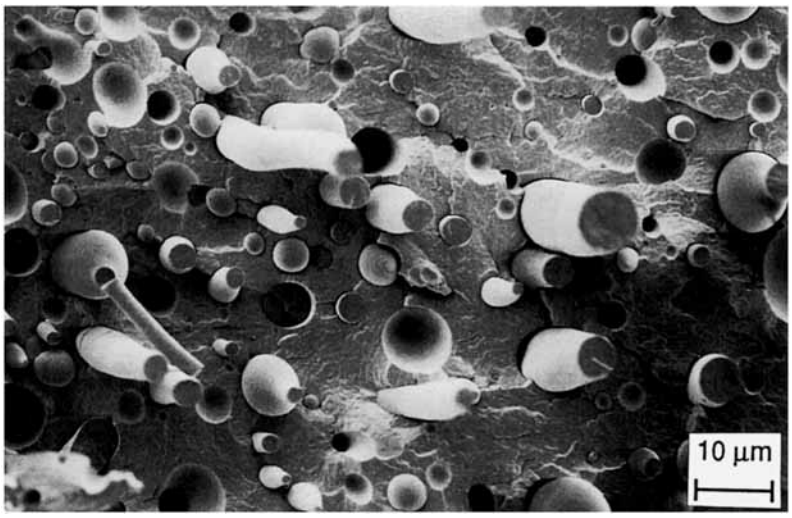

(B)

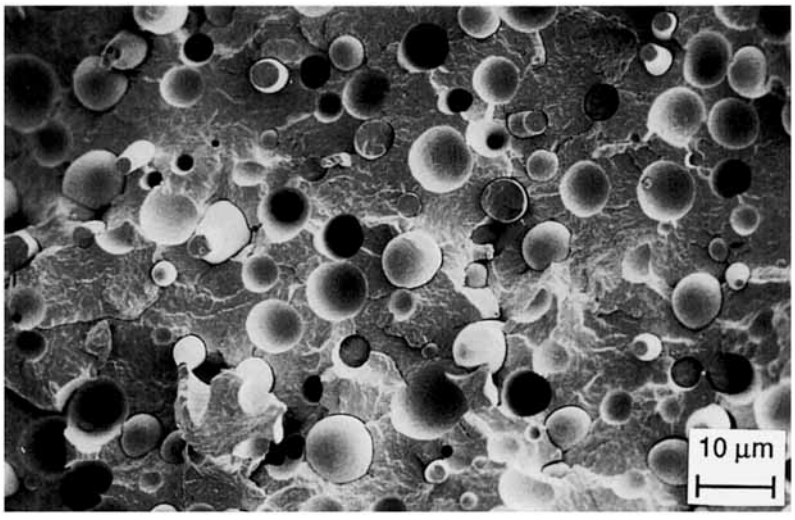

(C)

Figure 6 SEM photographs from blends (A) PA 80/PP VA4020E 20, (B) PA 80/PP VB6511B 20, (C) PA 80/PP VC1812H 20, (D) PA 80/PP VC3512H 20, and (E) PA 80/PP VC5076ENA 20.

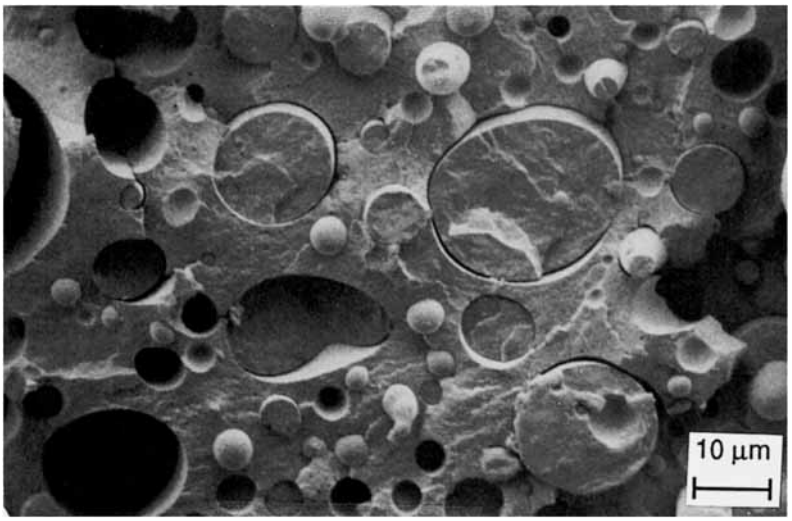

(D)

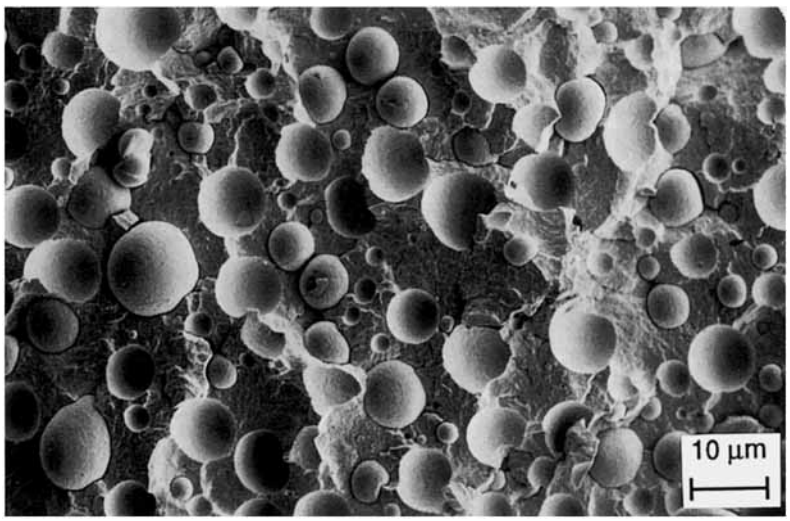

(E)

Figure 6 (*Continued from the previous page*)

shear rates studied. In extrusion, the shear rate varies in the range 100–1000 s^{-1}, and in injection molding, from 1000 to 10,000 s^{-1}.[12] Because it was difficult to determine any exact shear rate for the applied processing conditions, we selected the shear rate 200 s^{-1}, calculated by the method of Heidemeyer,[13] for the further consideration of the results. This value is assumed to best describe the average shear rate during the twin-screw extrusion.

Effect of Viscosity Ratio on the Phase Inversion

Noncompatibilized Blends

Morphology of the noncompatibilized blends was so coarse that the phase inversion could be determined with the help of an optical microscope and hot stage. The melting of the individual phases was observed, and whether the melting first took place in the dispersed particles or in the matrix was clarified.

The morphology was noticeably different in the blends of the most viscous PP, i.e., VA4020E. Instead of normal dispersion, islandlike structures and dual-phase continuity at PA concentrations 40 and 50 wt % were seen, perhaps indicating that the mixing procedure employed was not adequate for this grade.

The phase-inversion behavior of the noncompatibilized blends is depicted in Figure 2(a). The viscosity ratio was determined from Figure 1 at the estimated average shear rate 200 s^{-1}. The smaller the viscosity ratio, the smaller the PA concentration at which phase inversion occurred. However, the ef-

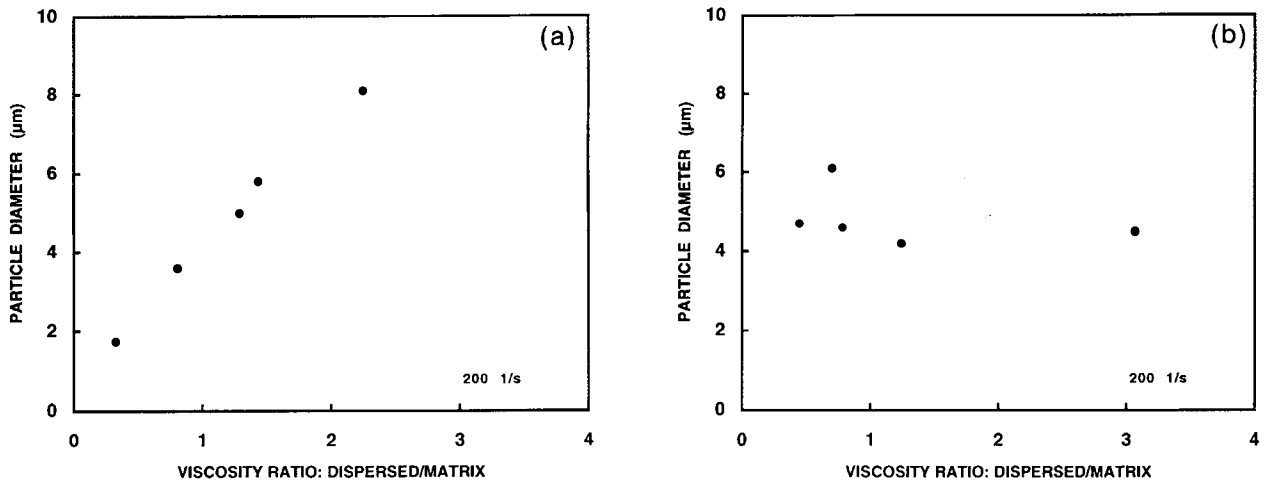

Figure 7 Dependence of the number-average diameter on the viscosity ratio ($\dot{\gamma}$ = 200 s^{-1}) of the noncompatibilized blends containing (a) 20 wt % PA or (b) 20 wt % PP dispersed in a matrix.

fect of viscosity ratio on the phase inversion was limited.

Compatibilized Blends

PP-*g*-MAH is an efficient compatibilizer and therefore the morphology of the compatibilized blends is below the threshold of the optical microscope. Due to the good adhesion, even SEM was not applicable. We therefore used TEM to define the phase-inversion regions of the compatibilized blends. PA was identified on the basis of its characteristic spherulite structure, and PP, on the basis of its lamellar structure.

The phase-inversion behavior of the compatibilized blends is depicted in Figure 2(b). The viscosity ratio was determined from Figure 1 at the estimated shear rate 200 s^{-1}. Addition of the compatibilizer changed the phase-inversion range only for the PA/PP VA4020E blends. In that case, dual-phase continuity was seen at a PA concentration 30 wt %. Evidently, it seems to us that the compatibilization achieved with PP-*g*-MAH does not have a pronounced effect on the composition of phase inversion.

Jordhamo et al.[14] developed an empirical model, based on the melt-viscosity ratio and volume fractions, for predicting the phase-inversion region of immiscible polymer blends. According to the model, phase inversion occurs when the following equation holds:

$$\frac{\eta_m}{\eta_d}\frac{\phi_d}{\phi_m} = 1 \qquad (2)$$

The quantities η_m and η_d represent the viscosities of the matrix and the dispersed phase, whereas ϕ_m and ϕ_d represent the volume fractions of the phases. Jordhamo's model is limited to low shear rates. The phase behavior according to the model is added to Figure 2(a) and (b). Our results at the shear rate 200 s^{-1}, which was chosen as an estimate the shear rate of a twin-screw extruder, correlate fairly well with the model. If a higher value of the shear rate is chosen, the correlation between the observed phase-inversion composition and the Jordhamo equation becomes weaker, in agreement with some previous investigations.[15,16]

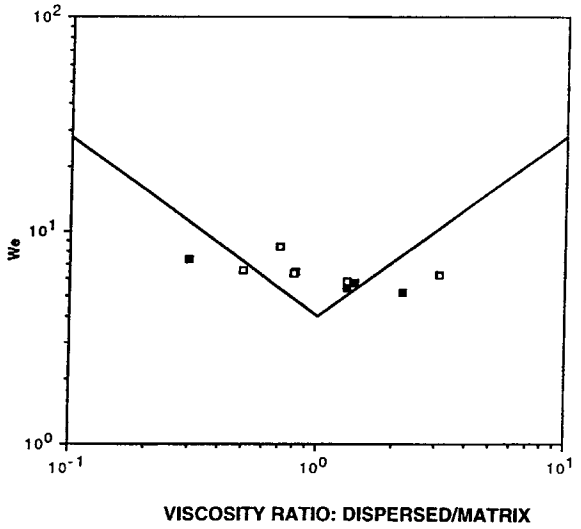

Figure 8 Dimensionless curve of Weber number vs. viscosity ratio ($\dot{\gamma}$ = 200 s^{-1}). Dispersed phase is (■) PA or (□) PP. Wu's curve is (-).

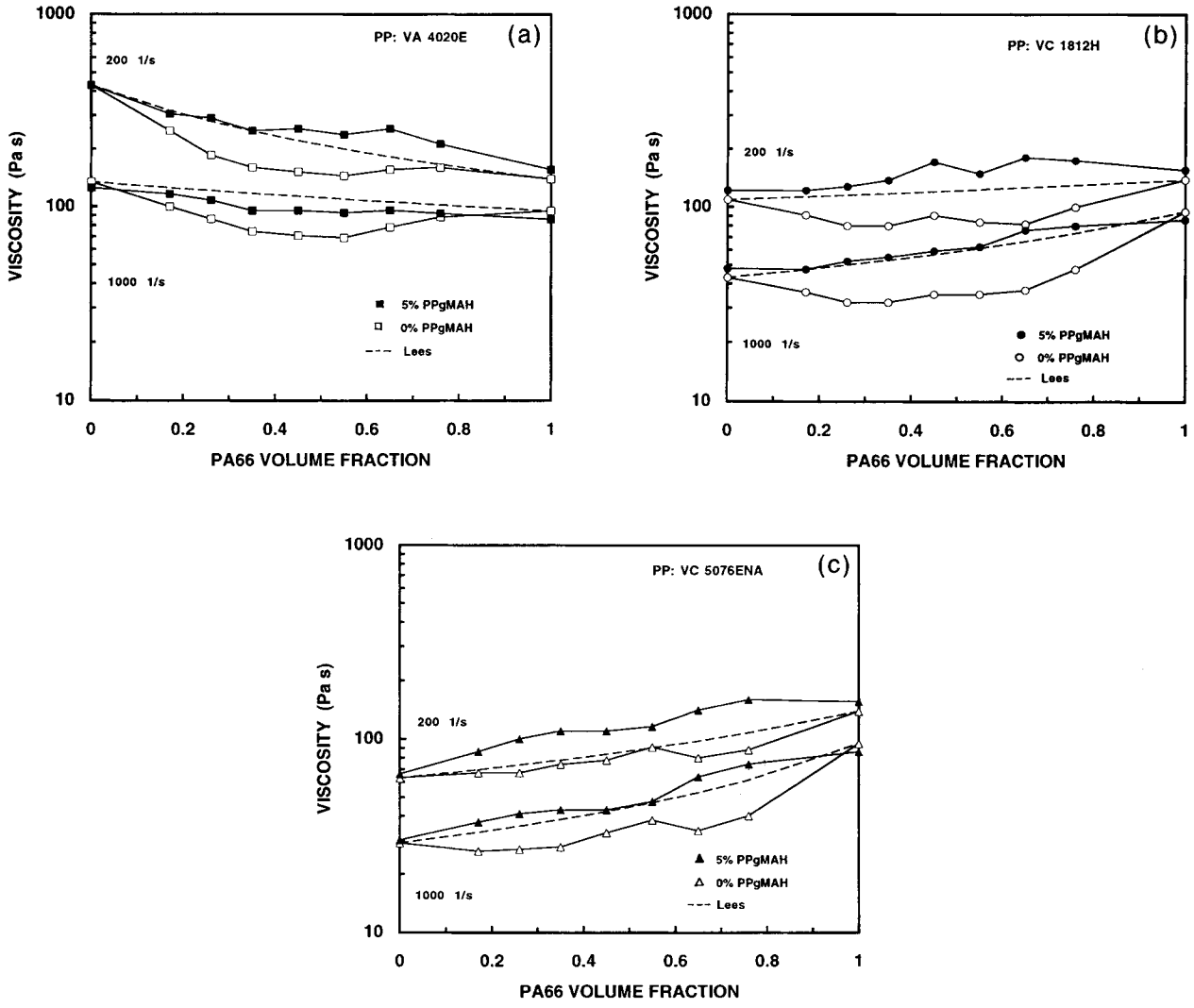

Figure 9 Composition dependence of the viscosities for (A) PA/PP VA4020E (B) PA/PP VC1812H, and (C) PA/PP VC5076ENA blends containing 0 and 5 wt % compatibilizer.

Interpretation of the morphology of some of the blends was complicated by the double dispersion: Inside the dispersed particles, there was a second dispersion. From TEM micrographs, we concluded that this second dispersion was composed of was the same material as that of the continuous phase. This unusual morphology may have been due to incomplete mixing.

Effect of Phase Inversion on the Mechanical Properties of the Compatibilized Blends

Mechanical and thermal properties of blends are expected to be determined mainly by the continuous phase. Improvement in the mechanical properties as a function of PA concentration may take place when the continuous PP phase is replaced by the continuous PA phase. Maximum tensile, flexural, and impact strength were investigated for two cases—PA/PP VC1812H and PA/PP VC5076ENA—as a function of the PA66 weight fraction.

The results of the maximum tensile strength measurements are summarized in Figure 3. The notched Izod impact strengths of the compatibilized predried samples are depicted in Figure 4. There was a clear dependence of toughness on the composition. The impact strength was better in blends where the PA weight fraction was 0.8 than in pure PA with the same amount of compatibilizer. The role of the dispersed PP is therefore essential. Earlier we noted this same behavior in PA/PP blends where an MAH-grafted styrene block copolymer was used

as the compatibilizer.[17] The impact properties are generally improved when the continuous PP phase is replaced by the continuous PA phase.

Morphology

Effect of Viscosity Ratio on the Size of the Dispersed Particles

The addition of compatibilizer changed the morphology of the blends considerably. The dispersion was too fine for the measurement of individual particle sizes from SEM micrographs and the use of TEM would have been required. Particle sizes were therefore determined only for noncompatibilized blends.

The average particle size of the dispersed phase was measured manually in noncompatibilized blends of composition PA20/PP80 and PA80/PP20. Typical SEM pictures are shown in Figures 5 and 6. On average, 300 measurements of the diameter were made for each sample. The number-average particle size as a function of the viscosity ratio is depicted in Figure 7. At the composition PA20/PP80, PA was the dispersed phase. The number-average particle size increased linearly from 1.7 μm at $p = 0.3$ to 8.1 μm at $p = 2.2$, which is in accordance with other studies of the dependence of the polymer blend morphology on torque or the viscosity ratio.[6,8,9,18] In PA80/PP20 blends, PP was the dispersed phase. In this case, no clear correlation between viscosity ratio and particle size was observed. The number-average particle size varied from 4.2 to 6.1 μm in the viscosity ratio range 0.5–3.1.

The approach of Wu suggests that there is a critical Weber number for each polymer pair below which dispersed particles will not deform. According to eq. (1), this critical Weber number is dependent only on the rheological properties of the components. Figure 8 plots the critical Weber number vs. viscosity ratio. Our data points fall near to Wu's master curve [eq. (1)]. However, the correlation between our results and Wu's equation is only approximate since we had only a few data points and the range of the viscosity ratio was narrow. The viscosity ratio was determined at the shear rate of 200 s^{-1}.

Rheology of the Blends

The rheological properties of a blend are associated with the phase morphology. A simple approach is to consider the mean shear rate in a volume element as the sum of the rates of the individual fractions:[19,20]

$$\dot{\gamma} = \phi_m \dot{\gamma}_m + \phi_d \dot{\gamma}_d \quad (3)$$

On the assumption that the stresses will be the same in all layers, the viscosity of the blend can be expressed as

$$\frac{1}{\eta} = \frac{\phi_m}{\eta_m} + \frac{\phi_d}{\eta_d} \quad (4)$$

This model, developed by Lee, predicts a monotonic variation of the reciprocal viscosity with volume fraction.

Figure 9 depicts the viscosity measured by capillary rheometer as a function of PA66 volume fraction at two shear rates. In noncompatible blends, viscosities showed a negative deviation from Lee's rule, indicative of incompatibility of the blends.[21] In the case of compatibilized blends, viscosities increased over the entire composition range. Only the pure components with the compatibilizer provided an exception. The viscosity–composition curves showed a clear positive deviation at shear rate of 200 s^{-1} and became more negative at a high shear rate (1000 s^{-1}). Similar viscosity–composition dependencies have been reported by Park et al.[22] The increase in viscosities demonstrates the reduction in interfacial mobility, caused by the chemical reaction between the amine end group of PA and the MAH group of the grafted PP.[9,22]

SUMMARY

The viscosity ratio in PA66/PP blends had only a limited effect on the phase inversion. Jordhamo's model[14] can be used to predict the continuous phase. Compatibilization of the blends with PP-*g*-MAH did not cause any significant change in the phase-inversion point, although the average particle size was greatly reduced.

Correlations were formed between mechanical properties of the compatibilized blends and phase inversion. In particular, the impact strength appears to critically depend on the continuous phase.

Our thanks to Ilkka Reima for his expertise in microscopy and to Kati Taskinen for assistance in the blending and testing.

NOMENCLATURE

PA	polyamide
PP	polypropylene

PP-*g*-MAH	maleic anhydride-grafted polypropylene
SEM	scanning electron microscopy
TEM	transmission electron microscopy

Symbols

p	viscosity ratio
r	radius of the particle (m)
We	Weber number
$\dot{\gamma}$	shear rate (s^{-1})
$\dot{\gamma}_d$	shear rate of the dispersed phase (s^{-1})
$\dot{\gamma}_m$	shear rate of the continuous phase (s^{-1})
γ_{12}	interfacial tension (mN/m)
η_i	viscosity of the polymer i (Pas)
η_d	viscosity of the dispersed phase (Pas)
η_m	viscosity of the continuous phase (Pas)
ϕ_d	volume fraction of the dispersed phase
ϕ_m	volume fraction of the continuous phase

REFERENCES

1. L. A. Utracki, *Polymer Alloys and Blends,* Carl Hanser Verlag, New York, 1990.
2. B. D. Favis and J. M. Willis, *J. Polym. Sci. Part B Polym. Phys.,* **28,** 2259 (1990).
3. K. Min, J. L. White, and J. F. Fellers, *Polym. Eng. Sci.,* **24,** 1327 (1984).
4. J. L. White and K. Min, *Adv. Polym. Tech.,* **5,** 225 (1985).
5. D. R. Paul and J. W. Barlow, *J. Macromol. Sci.-Rev. Macromol. Chem. C,* **18,** 145 (1980).
6. S. Wu, *Polym. Eng. Sci.,* **27,** 335 (1987).
7. G. Serpe, J. Jarrin, and F. Dawans, *Polym. Eng. Sci.,* **30,** 523 (1990).
8. B. D. Favis and J. P. Chalifoux, *Polym. Eng. Sci.,* **27,** 1591 (1987).
9. B. D. Favis and D. Therrien, *COMPALLOY'90,* 59 (1990).
10. J. M. Willis, V. Caldas, and B. D. Favis, *J. Mater. Sci.,* **26,** 4742 (1991).
11. S. S. Dagli, M. Xanthos, and J. A. Biesenberger, *COMPALLOY'91,* 257 (1991).
12. M. H. Pahl, *Praktische Rheologie der Kunststoffschmelzen und Lösungenen,* VDI-Verlag, Düsseldorf, 1983.
13. P. K. H. Heidemeyer, PhD Dissertation, Rheinisch-Westfälischen Technischen Hochschule, Aachen, 1990.
14. G. M. Jordhamo, J. A. Manson, and L. H. Sperling, *Polym. Eng. Sci.,* **26,** 517 (1986).
15. R. M. Ho, C. H. Wu, and A. C. Su, *Polym. Eng. Sci.,* **30,** 511 (1990).
16. I. S. Miles and A. Zurek, *Polym. Eng. Sci.,* **28,** 796 (1988).
17. R. Holsti-Miettinen, J. Seppälä, and O. T. Ikkala, *Polym. Eng. Sci.,* **32,** 868 (1992).
18. J. Karger-Kocsis, A. Kallo, and V. N. Kuleznev, *Polymer,* **25,** 279 (1984).
19. C. Lees, *Proc. Phys. Soc.,* **17,** 460 (1900).
20. R. F. Heitmiller, R. Z. Naar, and H. H. Zabusky, *J. Appl. Polym. Sci.,* **8,** 873 (1964).
21. B.-R. Liang, J. L. White, J. E. Spruiell, and B. C. Goswami, *J. Appl. Polym. Sci.,* **28,** 2011 (1983).
22. S. J. Park, B. K. Kim, and H. M. Jeong, *Eur. Polym. J.,* **26,** 131 (1990).

Received July 12, 1993
Accepted May 26, 1994